# Molecular Weight Effects in the Hydrogenation of Model Polystyrenes Using Platinum Supported on Wide-Pore Silica

**Jason S. Ness,[†] Jason C. Brodil,[†,‡] Frank S. Bates,[§] Stephen F. Hahn,[⊥] Dennis A. Hucul,[⊥] and Marc A. Hillmyer*[,†]**

*Department of Chemistry, University of Minnesota, Minneapolis, Minnesota 55455; Department of Chemical Engineering and Materials Science, University of Minnesota, Minneapolis, Minnesota 55455; and The Dow Chemical Company, Corporate Research and Development, Midland, Michigan 48674*

*Received June 1, 2001; Revised Manuscript Received October 31, 2001*

ABSTRACT: A kinetic study of the heterogeneous catalytic hydrogenation of model polystyrenes (PS) using a catalyst comprised of Pt on a wide-pore silica support was performed. The effect of molecular weight on the initial rate of hydrogenation, $r_0$, was investigated under conditions where mass transfer limitations were minimized. The $r_0$ values for a series of model polystyrenes ranging in molecular weight from 1.5 to 276 kg/mol were measured by monitoring hydrogen uptake with a digital mass flow controller. The initial rate of hydrogenation was found to be inversely proportional to PS molecular weight. For molecular weights up to 102 kg/mol, $r_0$ scaled with the number-average degree of polymerization, $\bar{X}_n$, to the −0.15 power. The two highest molecular weight samples, 190 and 276 kg/mol, exhibited significantly slower initial rates of hydrogenation and did not follow this trend. These results are explained in terms of equilibrium structure and conformational dynamics of a polymer on a metal surface and the relative dimensions of the polymer coils and Pt crystallites.

## Introduction

The hydrogenation of unsaturated polymers continues to be a widely used method for the preparation of thermally and oxidatively stable commercial materials (e.g., Kraton-G[1]) and model polyolefins.[2−4] The addition of hydrogen across olefins or aromatic residues in or along the polymer backbone can be accomplished by a variety of methods.[1,5−10] Although stoichiometric hydrogenations are effective,[7,11,12] catalytic addition of molecular hydrogen is preferred for both economical and technical reasons. Homogeneous catalytic systems, using soluble transition-metal complexes, can provide high activity and selectivity under mild reaction conditions, and mechanistic details have been uncovered in several systems.[5,13−16] Heterogeneous catalytic hydrogenation of unsaturated polymers typically requires the use of a supported noble metal catalyst, high $H_2$ pressures, and specialized equipment.[17] Catalyst separation, catalyst reusability, absence of metal contamination in the product, and low occurrence of polymer chain scission are all benefits that make heterogeneous methods desirable.[5,18] The heterogeneous hydrogenation of unsaturated polymers faces the same mechanistic challenges found in small molecule systems (e.g., hydrogenation of benzene or ethylene over Pt or Pd),[19−22] but the long chain nature of polymers leads to another degree of complexity not encountered in small molecules. The large size of typical unsaturated polymers can restrict their accessibility to the catalytically active sites on the support and can hinder the complete adsorption/reaction of the repeat units.

In 1984, Schulz and Worsfold examined the mechanism of the heterogeneous hydrogenation of polyisoprene (PI) with palladium supported on calcium carbonate ($Pd/CaCO_3$) at 25 °C and 14 psig of $H_2$.[8] Using $^{13}C$ NMR measurements and degradation experiments, they determined that hydrogenation of the PI chain occurs in a blocky manner; large sequences of carbon−carbon double bonds were hydrogenated in a single step before the polymer desorbed from the catalyst surface.[8] From their results, the hydrogenation appeared to occur in two distinct steps: the hydrogenation of a large fraction of the chain in the first step followed by a second adsorption/hydrogenation step. In 1988, Rosedale and Bates confirmed this blocky hydrogenation hypothesis in a study of 1,2-polybutadiene hydrogenation with $Pd/CaCO_3$ at 70 °C and 500 psig of $H_2$.[9] They proposed that the hydrogenation of the polybutadiene proceeds concomitantly with chain conformational rearrangement in a single adsorption step until about 85% of the chain has reached saturation. The thermodynamic driving force for chain adsorption at the catalytically active surface is sufficiently reduced at about 85% saturation that the chain desorbs, and further adsorption/hydrogenation steps are necessary to achieve complete conversion.[9] In subsequent studies using a similar system, the kinetics of hydrogenation were found to follow a two-step process as well: a fast initial rate (hydrogenation up to approximately 85% conversion) followed by a slower rate for the conversion of the remaining olefinic residues.[23] A 1998 study of 1,4-polybutadiene hydrogenation by Cassano et al. further supported this two-step mechanism.[24] Finally, Nakatani et al. showed partially hydrogenated samples of atactic polystyrene exhibit phase-separated morphologies, suggesting that some polymer chains are largely hydrogenated while others remain unsaturated (i.e., hydrogenation proceeds in a blocky fashion).[25]

While the hydrogenation of polydienes is relatively straightforward, the hydrogenation of polystyrenes requires more rigorous conditions (i.e., higher temperatures and pressures) and can be complicated by side

* To whom correspondence should be addressed. E-mail hillmyer@chem.umn.edu.
† Department of Chemistry, University of Minnesota.
§ Department of Chemical Engineering and Materials Science, University of Minnesota.
⊥ The Dow Chemical Company.
‡ Current address: The Dow Chemical Company, Midland, MI 48674.

10.1021/ma010960l CCC: $22.00 
Published on Web 12/21/2001

reactions. For instance, Gehlsen et al. reported that severe chain degradation and conversions of only 50% occurred in the hydrogenation of poly(α-methylstyrene).[10] Similarly, the hydrogenation of 330 and 560 kg/mol polystyrene (PS) samples using $Pd/BaSO_4$ was accompanied by chain degradation unless a small amount of THF was added to the cyclohexane solvent to increase PS solubility.[10] However, with the above exceptions, Gehlsen et al. were generally able to achieve quantitative PS hydrogenation in the absence of chain degradation using $Pd/BaSO_4$ and cyclohexane.[10] Through kinetic studies they identified five major variables that affect the hydrogenation process: external mass transfer, reaction temperature, type of catalyst support, polymer type, and polymer molecular weight.[23] Unfortunately, extraordinary amounts of catalyst were needed for appreciable hydrogenation rates. For example, Gehlsen et al. used 5 g of $Pd/BaSO_4$ per gram PS to achieve quantitative conversion to poly(cyclohexylethylene) (PCHE) in about 12 h.[10] This excessive amount of catalyst limits the utility of these catalysts. Of the variables that influence the hydrogenation process, the nature of the catalyst support can be particularly important.

Porous supports such as silica and alumina typically have very high surface areas (e.g., 200−600 $m^2/g$ for $SiO_2$) and consequently small average pore diameters (2−4 nm for $SiO_2$).[26] Increased support surface area leads to better metal dispersions and therefore higher rates of small molecule heterogeneous catalytic transformations. However, the reduction in pore size that accompanies the higher surface area supports can limit the access of unsaturated polymers to the catalytically active sites. As a result of this size exclusion, rates of polymer hydrogenation using high surface area porous supports are generally *slower* than by low surface area nonporous supports (e.g., alkaline metal salt supports < 50 $m^2/g$).[23,27] On the other hand, if the surface area of the support becomes too low, the "pore sizes" become macroscopic, and in the limit of bulk metal the surface area per gram of material is too small to exhibit appreciable hydrogenation activity.[28] It follows that in order to maximize the hydrogenation rate a balance is needed between the amount of catalytically active surface area (i.e., metal loading and dispersion) and pore sizes. Ideally, a support combining high enough surface areas to permit significant metal loadings and dispersions with pore sizes large enough to allow polymer access is desired.

Recently, the Dow Chemical Company has developed silica-supported Pt catalysts with large pore sizes and narrow pore size distributions.[26,29,30] A typical Dow hydrogenation catalyst (DHC) consists of 5 wt % Pt deposited on a wide-pore silica support as a 12% dispersion (i.e., 12% of all Pt atoms are on the surface of the Pt crystallites). The silica support has a surface area of about 15 $m^2/g$ with average pore sizes between 300 and 400 nm, with 98% of the pore volume being defined by pores having a diameter greater than 60 nm.[26] These large pore sizes allow the polymer chains access to the catalytically active sites within the pores, as a typical 100 kg/mol PS coil in solution has a radius of gyration of about 10 nm. The catalytic activity of DHC is significantly higher than the conventional nonporous supported catalysts.[31] Therefore, the quantity of DHC needed to hydrogenate a given mass of polymer is greatly reduced, making this catalyst far superior to the traditional $CaCO_3$ or $BaSO_4$ supported derivatives.

A fundamental understanding of the hydrogenation process using these novel catalysts is warranted. As such, we investigated the hydrogenation kinetics using a Pt catalyst on a wide-pore silica support (DHC) and model PS substrates. We monitored the hydrogen uptake using a digital mass flow controller and converted this into an initial rate of hydrogenation, $r_0$, at fixed reaction temperature, hydrogen pressure, and PS and catalyst concentration for seven model PS samples of varying molecular weight from 1.5 to 276 kg/mol.

## Experimental Section

**General Methods.** All hydrogenation reactions were performed in a Pressure Products Industries 300 mL baffled, high-pressure reactor with a Dyna/Mag magnetic drive mixer and a gas dispersion impeller. All anionic polymerizations were completed using standard Schlenk line techniques under inert argon atmosphere and high vacuum capable of $<10^{-3}$ Torr. $^1H$ NMR spectra of polymer samples in deuterated chloroform (Cambridge) were recorded on a Varian 500 VI spectrometer. Size exclusion chromatography analyses were performed on a Hewlett-Packard 1100 series liquid chromatograph equipped with a Hewlett-Packard 1047A refractive index detector and three Jordi poly(divinylbenzene) columns of $10^4$, $10^3$, and 500 Å pore sizes with THF as the mobile phase (40 °C and 1 mL/min). Column calibration was performed with polystyrene standards (Polymer Laboratories). UV analyses were performed on a Spectronic Instruments Genesys 5 spectrophotometer. All polymers were measured as solutions in THF (≈1−5 mg/mL) at a wavelength of 259 nm in Fisherbrand 10 mm path length (3 mL capacity) Suprasil quartz cells. Ultraviolet calibration curves were prepared for each polymer by measuring the UV absorbance of six polystyrene/THF solutions at concentrations ranging from 0 to 1.0 mg/mL. The calibration curve was modeled with a linear fit and used for the determination of percent conversion of polystyrene (PS) to poly(cyclohexylethylene) (PCHE). All kinetic measurements were performed with a Brooks Instrument Smart mass flow controller 5850S with a flow range of 5−500 sccm, using Smart DDE software for digital output. Galbraith Laboratories Inc., Knoxville, TN, performed all elemental analyses.

**Materials.** Commercial solvents and reagents were used as received without further purification except as noted. Styrene (Aldrich, 99%) was stirred over calcium hydride (Aldrich, 40 mesh, 90−95%) for at least 12 h at room temperature and distilled into a flask containing neat dibutylmagnesium (from a 1.0 M solution in heptane, Aldrich). The styrene was stirred over dibutylmagnesium for 4 h at room temperature and then distilled into a flame-dried buret. The concentration of *sec*-butyllithium (Aldrich, 1.3 M cyclohexane) was determined by the Gilman double-titration method.[32] Degassed cyclohexane for anionic polymerization and hydrogenation was rigorously purified by passage through an activated alumina column (LaRoche) for the removal of protic impurities and through a supported copper catalyst (Engelhard) to scavenge trace oxygen using a home-built solvent purification line.[33] This solvent purification system was interfaced with a Schlenk manifold to allow for anhydrous/anaerobic collection. Silica-supported platinum catalyst (Dow Chemical Company) was used as is unless otherwise specified. Hydrogen gas used for hydrogenation was ultrahigh-purity grade (99.995%) and was used without further purification.

**Synthesis of Polystyrene.** A general anionic polymerization procedure for the synthesis of 110 g of 100 kg/mol polystyrene is described below. Polymerization was performed in a 2 L round-bottomed glass reactor equipped with five internal Ace-Thred threaded glass connectors and a Teflon-coated stir bar. Using no. 15 Ace-Thred nylon bushings with FETFE O-rings, the reactor was fitted with three glass plugs, a glass thermowell, and a glass 90° connector. The glass 90° connector was equipped with three ports. Two ports were fitted

**Table 1. Sample Characterization and Average Initial Rate of Hydrogenation Results**

| polymer ID | $\bar{M}_n$ (kg/mol)[a] | $\bar{M}_n$ (kg/mol)[b] | PDI[b] | $10^4 r_0$ (mol/(L·s))[c] | TON[d] | $2R_g$[e] (nm) | $(\bar{D}_p/2R_g)$[f] | ([c]/[c*])[g] |
|---|---|---|---|---|---|---|---|---|
| PS-1 | 1.4 | 1.5 | 1.09 | 2.95 | 5.5 | 1.9 | 160 | 0.06 |
| PS-5 | 5.0 | 4.5 | 1.03 | 2.17 | 4.0 | 3.6 | 83 | 0.15 |
| PS-25 | 25 | 21 | 1.04 | 1.79 | 3.3 | 9.0 | 33 | 0.50 |
| PS-50 | 50 | 48 | 1.04 | 1.63 | 3.0 | 15 | 21 | 1.01 |
| PS-100 | 100 | 102 | 1.07 | 1.52 | 2.8 | 23 | 13 | 1.66 |
| PS-200 | 200 | 190 | 1.08 | 0.96 | 1.8 | 33 | 9.0 | 2.61 |
| PS-300 | 300 | 276 | 1.20 | 0.33 | 0.61 | 42 | 7.2 | 3.34 |

[a] Determined by reaction stoichiometry. [b] Determined by SEC vs PS standards. [c] Average initial rate, determined by evaluating the derivative of a second-order polynomial fit of a plot of $[S]_t$ vs $t$, at $t = 0$. [d] Turnover number, molecules of aromatic rings reacted per Pt site per second, from $\bar{r}_0$, at 170 °C and 500 psig of $H_2$ (based on $6.5 \times 10^{18}$ Pt sites/0.35 g of DHC). [e] The $R_g$ of PS in toluene, a good solvent, calculated using eq 2. [f] 300 nm was used as the average pore diameter. [g] Ratio of the standard PS concentration, $[c] = 0.035$ g/mL, to the calculated critical polymer concentration $[c^*]$, from eq 3.

with Chemcap valves (Viton O-ring, 0−4 mm) and interfaced to a vacuum/argon manifold and a manometer. The third port was fitted with a no. 7 Ace-Thred nylon bushing and a Teflon-coated septum. The reactor was evacuated to ≈$10^{-3}$ Torr and heated to ≈260 °C overnight to remove any adsorbed $H_2O$. After the reactor cooled, an air-free flask containing purified cyclohexane (≈1 L) and a buret of purified styrene (110.1 g, 1.059 mol) were added. The cyclohexane was added to the reactor followed by the addition (using an airtight syringe) of *sec*-butyllithium (1.328 M cyclohexane, 829 μL, 1.101 mmol) through the Teflon-coated septum. After the cyclohexane/*sec*-butyllithium solution was equilibrated to ≈40 °C, the styrene was added over a period of several minutes at a steady rate. Upon the addition of styrene, the solution turned a light orange color indicative of the living polystyryl chain ends. The temperature was maintained at 45 °C for 4.5 h. The reaction was then quenched with excess degassed methanol (1.0 mL). The resulting polymer solution was vacuum filtered to remove lithium methoxide salts and poured into a 75/25 mixture of methanol/2-propanol where a white polystyrene precipitate immediately formed. The solvent layer was decanted off, and polystyrene was collected and dried overnight under vacuum at ≈100 °C. The isolation yield was 107.2 g (97.4%). Size exclusion chromatography (SEC) analysis gave $M_n = 102$ kg/mol and $M_w/M_n = 1.07$, which agreed very well with the targeted molecular weight ($M_n = 100.0$ kg/mol) predicted from the reaction stoichiometry. All polystyrenes were stored at room temperature.

**Hydrogenation of Polystyrene.** All polystyrene/cyclohexane solutions were purified through an activated alumina column prior to hydrogenation in order to remove polar impurities and residual lithium methoxide salts detrimental to the catalyst. This column purification reduced the lithium content in the polymer solutions to <10 ppm (elemental analysis). A general procedure for the heterogeneous hydrogenation is described below. 157.3 g of the purified polymer solution (7 g PS, 150.3 g cyclohexane) was added to a 300 mL high-pressure solution delivery vessel (SDV). 5.5 g of additional purified cyclohexane was added to the SDV to achieve standard conditions (7 g of PS, 155.8 g of cyclohexane, 4.3 wt % PS). The SDV was jacketed by three heating bands and attached, via $^1/_4$ in. stainless steel tubing, to the reactor through the dip tube outlet valve. The Dow catalyst ($Pt/SiO_2$, 0.35 g, 0.05 catalyst to PS weight ratio) was loaded into the reactor, and the reactor was sealed. The catalyst was heated to 100 °C under vacuum for at least 1 h. The catalyst was reduced by adding 100 psig of $H_2$ and continuing to heat at 100 °C for an additional hour. After catalyst reduction, the reactor was vented, flushed three times with argon, and left under 20 psig of argon at 100 °C. The solution in the SDV was degassed for 25 min via bubbling argon before being injected into the reactor with 150 psig of argon. The excess argon pressure was vented until the reactor pressure was ≈30 psig (cyclohexane vapor pressure). The reactor was heated to 170 °C while stirring at a speed of 1500 rpm. Once the reactor temperature had equilibrated at 170 °C (≈1.3 h), a small aliquot (≈2 mL) of solution was collected and filtered through a 0.22 μm filter into methanol. This aliquot was necessary in order to determine the amount, if any, of PS hydrogenation due to the presence of any residual hydrogen in the reactor not removed by the argon flushes. The gas inlet valve on the reactor was opened to a constant pressure of ≈500 psig of $H_2$. This signaled the start of the hydrogenation reaction, or time zero. The solution was allowed to react for 4 h. The $H_2$ gas inlet valve was closed, and the reactor was rapidly cooled, via water-cooling coils, to ≈80 °C where stirring was stopped and the hydrogen was vented. The reactor was purged with 80 psig of argon several times before finally being left under 80 psig of argon. A Millipore high-pressure filter (with 0.22 μm filter paper) was attached to the reactor via the dip tube outlet valve and the hydrogenated polymer solution filtered into 400 mL of methanol. The methanol was decanted off, and the precipitated polymer was dried in a vacuum oven for at least 12 h at ≈100−140 °C (depending on the polymer molecular weight).

**Kinetic Measurements of Hydrogenation.** A Brooks mass flow controller with digital output was utilized for all kinetic measurements. This instrument monitored the hydrogen uptake into the reactor by recording the instantaneous flow rate of hydrogen, $r_{H_2}$, in g/h every 30 s for 4 h. When the reactor was first opened to 500 psig of $H_2$ (while stirring at 1500 rpm), the digital mass flow controller was circumvented (via $^1/_4$ in. stainless steel tubing) until the reactor pressure gauge reached 500 psig. This process (a few seconds in duration) allowed for the dissolution of hydrogen into solution and ensured that the rate data collected were due only to hydrogen consumption. Immediately after the reactor pressure reached ≈500 psig of $H_2$, the $H_2$ was rerouted through the digital mass flow controller, and data acquisition was initiated. This rerouting process could conceivably be avoided by using a reactor setup where the reduced catalyst is added to a polymer solution presaturated with $H_2$ (e.g., using a catalyst "basket" design); however, the technical challenges associated with such a design were difficult to surmount. When $r_{H_2}$ had slowed to a value of ≈0.1 g/h, the extent of PS hydrogenation was high (generally >90%), so a small aliquot (≈2 mL) of solution was collected and filtered into methanol. This aliquot allows for the accurate correlation of percent hydrogenation with flow rate data. The accuracy of the digital mass flow controller employed begins to decrease significantly near $r_{H_2} \approx 0.1$ g/h, and therefore data with hydrogen consumption rates ≤0.1 g/h were not used in the determination of the initial rate of hydrogenation.

**Polymer $^1$H NMR Characterization.** The following sets of $^1$H NMR spectroscopy resonances are representative of the polystyrene and corresponding poly(cyclohexylethylene) samples described in this paper. All resonances are reported in ppm (δ) downfield from the internal reference tetramethylsilane (0.0 ppm), as either broad (b) or containing multiple overlapping peaks (m). Polystyrene: 1.20−1.65 (b, −C**H**$_2$−), 1.65−2.10 (b, ⟩C**H**−), 6.30−6.80 (b, =C**H**− ortho position), 6.80−7.20 (b, =C**H**− meta, para position). Poly(cyclohexylethylene): 0.65−1.0 (b −C**H**$_2$− and ⟩C**H**−), 1.0−2.0 (b, cyclic ⟩C**H**$_2$).

## Results and Discussion

The polystyrene homopolymers listed in Table 1 were prepared by anionic polymerization and are monodisperse ($\bar{M}_w/\bar{M}_n < 1.10$) with $\bar{M}_n$ as determined by size exclusion chromatography (SEC) close to the predicted

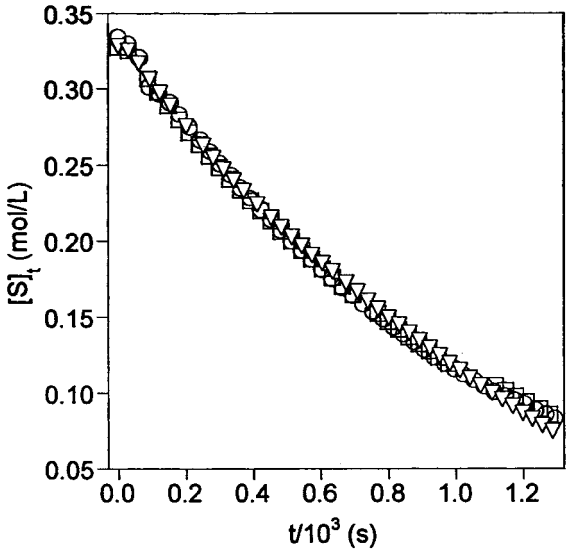


**Figure 1.** Determination of the average initial rate of hydrogenation for sample PS-1 (1.5 kg/mol). Kinetic plot showing the time dependence of the instantaneous styrene concentration for three hydrogenations using standard hydrogenation conditions of 4.3 wt % PS-1 in cyclohexane at 170 °C and 500 psig of $H_2$ for 4 h.

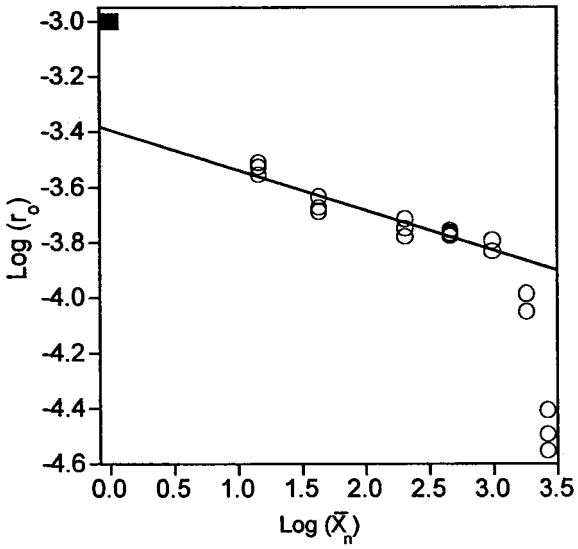


**Figure 2.** Dependence of the initial rate of hydrogenation on PS number-average degree of polymerization ($\bar{X}_n$). Samples PS-1 (1.5 kg/mol) through PS-100 (102 kg/mol) lie on the trendline shown. Samples PS-200 (190 kg/mol) and PS-300 (276 kg/mol) lie significantly below the trendline. Circles represent all PS samples. Also included in this plot is the estimated initial rate of hydrogenation for toluene, $\sim 10^{-3}$ mol/(L·s) (square).[51]

stoichiometric values. All hydrogenation reactions proceeded to near quantitative conversion (>99%) as evidenced by the absence of residual aromatic proton resonances near 7 ppm in the $^1$H NMR spectra and confirmed by UV spectroscopy (see Experimental Section).[34] The polydispersities of the hydrogenated products remained narrow, confirming that hydrogenation occurred in the absence of chain scission.

The initial rate of hydrogenation, $r_0$, for each of the PS samples was determined by measuring the instantaneous rate of $H_2$ consumption (at fixed temperature, $H_2$ pressure, and PS concentration) and converting that into the instantaneous concentration of aromatic rings, $[S]_t$ (in mol/L), which was then plotted against time. Representative data for three hydrogenations of sample PS-1 (1.5 kg/mol) are shown in Figure 1. Each plot included data up to two half-lives and was fit to a second-order polynomial.[35] The derivative of this polynomial with respect to time yielded a first-order expression, and the coefficient independent of time in this expression was used as $r_0$.[36] The average initial rate values, $\bar{r}_0$, for each molecular weight of PS (three trials)[37] are reported in Table 1. The initial rates decreased as PS molecular weight increased; $\bar{r}_0$ for PS-1 was nearly 10 times larger than for PS-300. A plot of log $r_0$ vs log $\bar{X}_n$ is shown in Figure 2. This plot gave the relationship $r_0 \propto \bar{X}_n^{-0.15}$ for samples PS-1 through PS-100. The two highest molecular weight samples, PS-200 and PS-300, have $r_0$ values significantly below this line.

The simplest explanation for the trend in Figure 2 is that mass transport limitations are influencing $r_0$; however, through the use of both specialized reactor equipment and experimentation, we found this not to be the case. Mass transport limitations include the external and internal diffusion (e.g., pore diffusion) of both $H_2$ and polymer. Gehlsen et al. demonstrated that $H_2$ external diffusion limitations could be eliminated through a combination of rigorous solution mixing (mixing speeds >500 rpm) and the use of a reactor fitted with baffles.[23,38] They showed that this set of conditions created forceful interfacial infusion of $H_2$ into the liquid phase, producing reaction rates free of external $H_2$ transport limitations.[23] In addition to utilizing identical mixing conditions, our reactor was equipped with a gas dispersion impeller allowing for even greater dissolution of $H_2$ into the liquid phase.[38] Therefore, the data presented here were obtained under conditions that minimized $H_2$ external transport.

To determine whether polymer external diffusion limitations were influencing $r_0$, a set of experiments were performed to elucidate the correlation between $r_0$, polymer concentration, and solution viscosity. An estimation of polymer solution viscosity, $\eta$, was made using a relationship between polymer concentration and molecular weight in the concentrated polymer solution regime (>1 wt % polymer), as shown in eq 1,[39]

$$\eta = Kc^{\alpha}M^{\beta} \tag{1}$$

where $K$ is a constant dependent on the nature of the polymer−solvent system, $c$ is the concentration in wt % polymer, and $M$ is polymer molecular weight. The exponent $\alpha$ has a mean value of 5.1, and $\beta$ has a value close to 3.4 (the value of the exponent in the relationship between viscosity and molecular weight in the melt).[39] Using this equation, solution viscosities for four PS-100 solutions (8.5, 6.3, and 4.3 wt % PS), two PS-200 solutions (4.3 wt % PS), and three PS-300 solutions (4.3 wt %) were calculated (we assumed $K$ was constant for all cases). The initial rates of hydrogenation for these solutions were then measured. To make certain that any effect on $r_0$ could be correlated to a change in solution viscosity only, the weight ratio of catalyst to PS was held constant at 0.05. We also determined (consistent with previous results by Gehlsen[23] and Weimann[38]) that $r_0$ is directly proportional to the mass of DHC.[40] Accordingly, each $r_0$ could be normalized by the mass of DHC used in order to separate dependence on increased catalyst concentrations from viscosity effects (as the reaction is first order with respect to [DHC]). Figure 3 shows a plot of $r_0/M_{DHC}$ (mass of DHC,

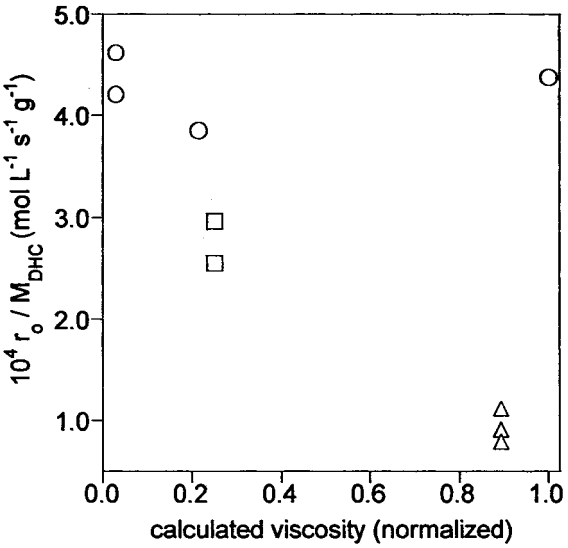


**Figure 3.** Dependence of the initial rate of hydrogenation (normalized by grams of DHC) on calculated solution viscosity (normalized by dividing by the most viscous solution, the 8.5 wt % PS-100 solution). PS-100 solutions (102 kg/mol, at 8.5, 6.3, and 4.3 wt %) as circles, PS-200 solutions (190 kg/mol at 4.3 wt %) as squares, and PS-300 solutions (276 kg/mol, at 4.3 wt %) as triangles.

in grams) vs the normalized calculated viscosity for four PS-100 solutions, two PS-200 solutions, and three PS-300 solutions. We normalized the calculated solution viscosities by dividing by the viscosity of the most viscous solution (8.5 wt % PS-100 solution). The solution viscosity for the PS-100 solutions appears to have no effect on the initial reaction rate. Furthermore, Figure 3 demonstrates that at the same calculated solution viscosity $r_0/M_{DHC}$ is slowest for the highest molecular weight PS (PS-300) even though this solution does not have the highest calculated viscosity. These results suggest that polymer external diffusion is not limiting the reaction kinetics.[41] This conclusion that solution viscosity has no effect on $r_0$ is valid only if the reaction order in [styrene] is approximately zero. If the reaction order in [styrene] is greater than zero, then increasing the [styrene] should also increase $r_0$. Yet no increase in $r_0$ was observed. In fact, at fixed catalyst concentration when the concentration of PS (≈100 kg/mol) was varied from 0.035 to 0.070 g/mL, $r_0$ actually decreased slightly from $1.52 \times 10^{-4}$ to $1.22 \times 10^{-4}$ mol/(L·s). This is suggestive of a reaction order in [styrene] near to zero. Furthermore, Singh and Vannice have shown that in the liquid-phase hydrogenation of benzene over Pd/$\eta$-$Al_2O_3$ (at 140 °C and 200 psig of $H_2$) the reaction order in [benzene] is 0−0.1.[20] These data are consistent with our conclusion that polymer diffusion is not limiting the reaction kinetics. However, internal or pore diffusion limitations could be influencing the observed reaction kinetics.

Kawaguchi et al. studied the adsorption of monodisperse PS chains at a well-defined porous silica surface with relatively narrow pore size distributions under Θ and good solvent conditions.[42−44] They found for a given solvent that more time was required for PS chains to reach adsorption equilibrium on porous silica relative to nonporous silica when the ratio of the average pore diameter to twice the radius of gyration ($R_g$) of the PS chain ($\bar{D}_p/2R_g$) was ≤2.5.[43,44] In such cases, the PS chain must significantly deform itself in order to penetrate the pores.[43,44] If such a phenomenon is occurring in our system, polymer pore diffusion could be an explanation for the trend shown in Figure 2.

To determine the $\bar{D}_p/2R_g$ ratio for our system, we needed to estimate the $R_g$ of PS in cyclohexane at 170 °C (a temperature above the Θ temperature, 34.5 °C). Melnichenko et al. studied the effect of temperature on the $R_g$ of PS in cyclohexane for a semiconcentrated solution.[45] They found above the Θ temperature this system exhibited a "good solvent" domain, meaning the molecules expanded beyond their unperturbed dimensions.[45] Although Melnichenko et al. did not investigate temperatures as high as 170 °C, we feel it is reasonable to assume (for the purposes of estimating $2R_g$) that $R_g$ will expand as it would in a good solvent. Therefore, eq 2 was used to determine the $R_g$ of PS in toluene.[46]

$$R_g^{tol} = 1.20 \times 10^{-2} M^{0.595} \qquad (2)$$

Using this equation and a value of 300 nm for the average pore diameter of the support, $\bar{D}_p/2R_g$ values representing a lower limit were obtained. The calculated results are shown in Table 1. All PS samples used in this study have size ratios significantly greater than 2.5. Even the largest PS sample (PS-300) has a size ratio of 7.2, nearly 3 times the ratio where polymer deformation becomes important, suggesting that the PS chains do not need to deform themselves in order to enter the pores. Therefore, pore diffusion limitations are unlikely to be the cause for the decrease in the initial rate of hydrogenation. Since neither external nor pore diffusion are presumably responsible for the inverse relationship between $\bar{r}_0$ and molecular weight (Figure 2), adsorption phenomena between the PS and Pt crystallites may be implicated.

Polymer adsorption onto metal surfaces is a complex process influenced by many factors including polymer chain length (i.e., $\bar{X}_n$), polymer−surface, solvent−surface, and polymer−solvent interactions.[9] In the case of PS and Pt, there is a strong thermodynamic driving force for the aromatic rings to chemisorb onto the Pt surface due to favorable interactions between the aromatic $\pi$ orbitals and the vacant metal orbitals to form a $\pi$-complex.[47] However, at sufficient molecular weight, entropic penalties prohibit the complete adsorption of an entire chain of aromatic units. Therefore, only small sections of the chain, called trains, adsorb and have the opportunity to be hydrogenated at any given time. Furthermore, the thermodynamic driving force for adsorption lessens as the chain becomes hydrogenated since the saturated cyclohexane rings prefer the solvent to the Pt surface. Scheutjens and Fleer, on the basis of a matrix model for polymer adsorption, have calculated the conformation of adsorbed chains at equilibrium.[48] They calculated the distribution and sizes of trains, loops, and tails as a function of chain length in Θ and athermal solvents ($\chi$ = 0.5 and 0, respectively), at a polymer volume fraction of 0.01, using a hexagonal lattice and an adsorption energy parameter, $\chi_s = 1$ (strong thermodynamic driving force for adsorption).[48] Our system is well represented by these conditions since PS in cyclohexane at 170 °C has $\chi < 0.5$, the PS volume fraction is 0.035, and the aromatic−Pt interaction is strong.

Theoretically,[48] as polymer chain length increases from $\bar{X}_n \approx 100$ to 1000, $n_{train}$ and $n_{loop}$ (the average number of trains and loops per chain, respectively) increase linearly and $n_{tail}$ (the average number of tails

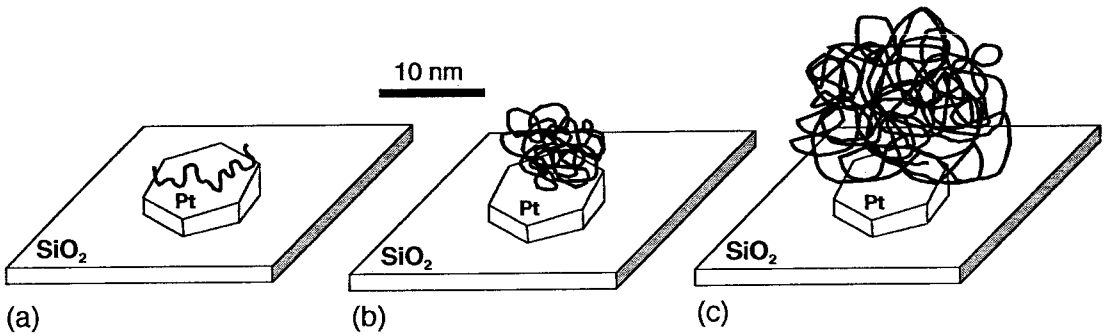


**Figure 4.** Schematic representation of PS hydrogenation on $Pt/SiO_2$ with an average Pt crystallite diameter of ≈10 nm. (a) Low-molecular-weight PS (e.g., PS-1). (b) Medium-molecular-weight PS (e.g., PS-50). (c) High-molecular-weight PS (e.g., PS-300). When the diameter of the PS coil is significantly larger than the average Pt crystallite (c), the rate of hydrogenation is considerably diminished (see Figure 2).

per chain) remains fairly constant. However, over the same range of $\bar{X}_n$, $l_{tail}$ (the average length of the tails) increases dramatically, while $l_{train}$ and $l_{loop}$ (the average length of the trains and loops, respectively) remain the same (with $l_{train} \approx 4$ repeat units). Similarly, as $\bar{X}_n$ increases from 100 to 1000, $\nu_{train}$ (the fraction of styrene units present as trains) decreases from 0.42 to 0.27, $\nu_{loop}$ (the fraction of styrene units present as loops) increases from 0.38 to 0.52, and $\nu_{tail}$ (the fraction of styrene units present as tails) remains constant at about 0.21. Thus, as $\bar{X}_n$ increases, the fraction of styrene units in loops increases at the expense of the fraction in trains.

Comparing PS-1 and PS-100 ($\bar{X}_n \approx 14$ and 980, respectively), we calculated $\nu_{train} \approx 0.66$, $\nu_{loop} \approx 0.17$, and $\nu_{tail} \approx 0.19$ for PS-1 and $\nu_{train} \approx 0.27$, $\nu_{loop} \approx 0.52$, and $\nu_{tail} \approx 0.21$ for PS-100. The PS-1 chain initially has on average 9 styrene units adsorbed on the catalyst surface while on average 2.4 and 2.6 units are in loops and tails, respectively. Thus, the majority of the chain is adsorbed on the catalyst surface and available for hydrogenation at once. On the other hand, PS-100 has approximately 265 out of 980 styrene units adsorbed on the Pt surface with the majority of its styrene units in loops and tails. Recall that Rosedale and Bates in their study of 1,2-polybutadiene hydrogenation concluded that about 85% of a 1,2-polybutadiene chain is hydrogenated in a single adsorption step.[9] They proposed that this required significant conformational rearrangement of the partially hydrogenated polymer chain on the catalyst surface (occurring concomitantly with hydrogenation) and that the chains were sufficiently dynamic to allow for this conformational rearrangement to occur.[9] Since a longer chain will need more conformational rearrangements to reach this high level of conversion in a single adsorption step, a slower $r_0$ (relative to a shorter chain) would be expected, as on average a larger polymer chain would occupy a catalyst site for a longer amount of time. This suggests that $r_0$ is a measure not only of the rate of the addition of hydrogen to an aromatic unit but also of the time necessary for the chains to conformationally rearrange while adsorbed on the Pt surface.

In the extreme case of a 1-mer or a single styrene unit, the entire molecule adsorbs on the Pt surface with as many molecules as possible adsorbing on a given Pt crystallite at once. As a result, $r_0$ should be very fast even in comparison to the lowest molecular weight polymer sample, PS-1. Under the same conditions as the PS substrates, the initial rate of hydrogenation for toluene (a model PS with $\bar{X}_n = 1$) was so fast that complete hydrogenation was achieved in a matter of minutes ($r_0 \sim 10^{-3}$ mol/(L s), see Figure 2).[51] For toluene hydrogenation, $r_0$ reflects only the rate of hydrogen addition to an aromatic residue, as there is no chain to conformationally rearrange. The effect of the polymer chain conformational rearrangement on the initial rate of hydrogenation is relatively weak, scaling as the number-average molecular weight to a factor of about $-0.15$ between $\bar{X}_n \approx 14$ and $\bar{X}_n \approx 980$.

The result that samples PS-200 and PS-300 have initial rates of hydrogenation much slower than the scaling factor ($\bar{X}_n^{-0.15}$) for PS-1 through PS-100 can be explained by considering two related factors: the size of these polymers relative to the size of a Pt crystallite and the effect of interchain interactions. Bates et al. measured the average Pt crystallite diameter of the DHC to be about 10 nm via transmission electron microscopy.[49] From Table 1, the diameters ($2R_g$) of PS-100, PS-200, and PS-300 are approximately 23, 33, and 42 nm, respectively, all larger than the diameter of a Pt crystallite. However, only the latter two samples, with approximate diameters 3 and 4 times that of a Pt crystallite, have initial rates of hydrogenation much slower than predicted by the relationship shown in Figure 2. Presumably, chains longer than PS-100 are too large for a given Pt crystallite to accommodate the adsorption of the train segments ($\nu_{train}$) all at once. Essentially, these chains are so big they spill over the sides of the Pt crystallite. The inability to adsorb the entire fraction of styrene segments present as trains increases the number of chain conformational rearrangements necessary to achieve high conversion during the first adsorption step, resulting in a slower $r_0$ (Figure 2). A catalyst with Pt crystallite sizes equal to or larger than the PS-200 and PS-300 chains should yield faster initial rates than observed with DHC.[50] Employing such a catalyst for the hydrogenation of PS-200 and PS-300 would be revealing and is worth exploring. Furthermore, it is expected that an increase in the reaction temperature would lead to an increase in $r_0$ due, in part, to an increase in the rate of conformational rearrangements, and preliminary examinations of $r_0$ at varying reaction temperatures support such a temperature dependence. However, increasing the temperature affects more than just the chain dynamics at the Pt surface. Chemical reaction rate, diffusion, and the partitioning of the polymer between the solution and the surface are all dependent on temperature, and their dependencies may be different; thus, deconvolution is challenging.

To determine whether interchain interactions are influencing the initial rates of hydrogenation for PS-200 and PS-300, we needed to establish whether these

polymer solutions were above the critical overlap concentration where interchain interactions become important, [*c**]. We calculated the ratio of the standard polymer solution concentration, [*c*], to the critical polymer concentration for all our PS samples. An estimate of [*c**] was made for a polymer in a good solvent using eq 3.

$$[c^*] = \frac{\phi_2 \bar{M}_w}{N_{av}\frac{4}{3}\pi R_g^3} \quad (3)$$

In this equation, $\phi_2$ is the volume fraction carved out by the polymer coil "spheres", $\bar{M}_w$ is the weight-average molecular weight, $N_{av}$ is Avogadro's number, and $R_g$ is the radius of gyration (see eq 2). For $\phi_2$, the value for a close packed system ($\phi_2 = 0.74$) was used, which represents the maximum packing fraction for close-packed spheres. Table 1 shows the calculated results. The concentrations of samples PS-1 through PS-25 are well below [*c**], the concentration of PS-50 is right at [*c**], and the concentrations of PS-100, PS-200, and PS-300 are above [*c**]. These results suggest that the polymer coils in the PS-100, PS-200, and PS-300 solutions interpenetrate to some degree. The result of this interchain overlap may be an increase in the number of chain conformational rearrangements required to reach high conversion during the first adsorption step and consequently a slower $r_0$.

## Summary

A kinetic study of the heterogeneous catalytic hydrogenation of model polystyrene (PS) using a catalyst comprised of Pt on a wide-pore silica support was performed. The effect of molecular weight on the initial rate of hydrogenation, $r_0$, was investigated under conditions where mass transfer limitations were minimized. The $r_0$ values for a series of anionically prepared polystyrenes ranging in molecular weight from 1.5 to 276 kg/mol were measured by monitoring hydrogen uptake with a digital mass flow controller at fixed conditions of 170 °C, 500 psig of $H_2$, 0.05 catalyst to PS weight ratio, and 4.3 wt % PS. All hydrogenations were performed in the absence of chain scission and achieved complete conversion (>99%). The initial rate of hydrogenation was found to be inversely proportional to the molecular weight of the PS. For molecular weights up to 102 kg/mol, $r_0$ scaled with the number-average degree of polymerization, $\bar{X}_n$, to the −0.15 power. The two highest molecular weight samples, 190 and 276 kg/mol, exhibited significantly slower initial rates of hydrogenation and did not follow this trend. These results were explained in terms of equilibrium structure and conformational dynamics of a polymer on a metal surface and the dimensions of the polymer coils and Pt crystallites.

**Acknowledgment.** We are grateful to the Dow Chemical Company for providing the hydrogenation catalyst and funding for this project.

## References and Notes

(1) McManus, N. T.; Rempel, G. L. *J. Macromol. Sci., Rev. Macromol. Chem. Phys.* **1995**, *C35*, 239.
(2) Bates, F. S.; Rosedale, J. H.; Bair, H. E.; Russell, T. P. *Macromolecules* **1989**, *22*, 2557.
(3) Douzinas, K. C.; Cohen, R. E.; Halaasa, R. E. *Macromolecules* **1991**, *24*, 4457.
(4) Kishnamoorti, R.; Graessley, W.; Balsaara, N. P.; Lohse, D. J. *Macromolecules* **1994**, *27*, 3073.
(5) Rachapudy, H.; Smith, G. G.; Raju, V. R.; Graessley, W. W. *J. Polym. Sci., Polym. Phys. Ed.* **1979**, *17*, 1211.
(6) Falk, J. C. *Makromol. Chem.* **1972**, *160*, 291.
(7) Nakagawa, T.; Okawara, M. *J. Polym. Sci., Part A-1* **1968**, *6*, 291.
(8) Schulz, G.; Worsfold, D. J. *Polym. Commun.* **1984**, *25*, 206.
(9) Rosedale, J. H.; Bates, F. S. *J. Am. Chem. Soc.* **1988**, *110*, 3542.
(10) Gehlsen, M. D.; Weimann, P. A.; Bates, F. S. *J. Polym. Sci., Part B: Polym. Phys.* **1995**, *33*, 1527.
(11) Edwards, H. G. M.; Farwell, D. W.; Johnson, A. F.; Lewis, I. R.; Ward, N. J.; Webb, N. *Macromolecules* **1992**, *25*, 525.
(12) Hahn, S. F. *J. Polym. Sci., Part A: Polym. Chem.* **1992**, *30*, 397.
(13) Guo, X.; Rempel, G. L. *J. Mol. Catal.* **1990**, *63*, 279.
(14) Guo, X.; Scott, P. J.; Rempel, G. L. *J. Mol. Catal.* **1992**, *72*, 193.
(15) Singha, N. K.; Sivaram, S. *Polym. Bull. (Berlin)* **1995**, *35*, 121.
(16) Mohammadi, N. A.; Rempel, G. L. *J. Mol. Catal.* **1989**, *50*, 259.
(17) Hillmyer, M. A. *Today's Chemist at Work* **1999**, *8*, 21.
(18) Gehlsen, M. D.; Bates, F. S. *Macromolecules* **1993**, *26*, 4122.
(19) Orozco, J. M.; Webb, G. *Appl. Catal.* **1983**, *6*, 67.
(20) Vannice, M. A.; Singh, U. K. *AIChE J.* **1999**, *45*, 1059.
(21) Zaera, F. *Langmuir* **1996**, *12*, 88.
(22) Vannice, M. A.; Poondi, D. *J. Catal.* **1996**, *161*, 742.
(23) Gehlsen, M. D. Ph.D. Thesis, University of Minnesota, Minneapolis, 1993.
(24) Cassano, G. A.; Valles, E. M.; Quinzani, L. M. *Polymer* **1998**, *39*, 5573.
(25) Nakatani, H.; Nitta, K.-h.; Soga, K. *Polymer* **1998**, *39*, 4273.
(26) Hucul, D. A.; Hahn, S. F. US Patent 5 654 253, 1997.
(27) Collman, J. P.; Kosydar, K. M.; Bressan, M.; Lamanna, W.; Garrett, T. *J. Am. Chem. Soc.* **1984**, *106*, 2569.
(28) The surface area of 500 mg of a thin Pt wire (0.076 mm diameter by 5 m long) is $2.4 \times 10^{-3}$ $m^2/g$.
(29) Hucul, D. A.; Hahn, S. F. US Patent 5 612 422, 1997.
(30) Hucul, D. A.; Hahn, S. F. *Adv. Mater.* **2000**, *12*, 1855.
(31) The higher activity results in part from the Pt metal itself, as Pt is known to have a higher activity than Pd in the hydrogenation of alkenes. See: Hartley, F. R. *The Chemistry of the Metal−Carbon Bond*; John Wiley and Sons: New York, 1987; Vol. 4.
(32) Gilman, H.; Cartledge, F. K. *J. Organomet. Chem.* **1964**, *2*, 447.
(33) Pangborn, A. B.; Giardello, A.; Grubbs, R. H.; Rosen, R. K.; Timmers, F. J. *J. Organomet. Chem.* **1996**, *15*, 1518.
(34) PS-300 had a final conversion of approximately 94%.
(35) The $[S]_t$ vs time plot for sample PS-300 only included data up to about 31% as this was the level of conversion at the time of sampling due to the slow hydrogenation rate.
(36) Espenson, J. H. *Chemical Kinetics and Reaction Mechanisms*, 2nd ed.; McGraw-Hill: New York, 1995.
(37) The average initial rate for PS-200 was based on only two trials.
(38) Weimann, P. A. Ph.D. Thesis, University of Minnesota, Minneapolis, 1998.
(39) VanKrevelen, D. W. *Properties of Polymers*, 3rd ed.; Elsevier Science: Amsterdam, 1997.
(40) For example, modifying the catalyst to PS ratio for PS-50 from 0.025 to 0.05 resulted in initial rates of 0.83 and $1.63 \times 10^{-4}$ mol/(L s), respectively. These results are consistent with previous results by Gehlsen and Weimann. See refs 23 and 38.
(41) The Madon−Boudart test can be used to determine whether effects due to mass transfer are influencing the observed reaction rate. In the kinetic regime, the reaction rate is directly proportional to the concentration of the catalytically active sites for a given mass of catalyst. This holds true provided that the reaction is structure-insensitive (i.e., not dependent on the surface structure of the active sites). See: Madon, R. J.; Boudart, M. *Ind. Eng. Chem. Fundam.* **1982**, 21. Boudart, M. *Adv. Catal.* **1969**, *20*, 153. Unfortunately, the hydrogenations performed in our study were structure-sensitive, and therefore we were not able to use this technique.
(42) The adsorption isotherms for the individual PS chains were of the high affinity type, i.e., favorable chain adsorption.
(43) Kawaguchi, M.; Anada, S.; Nishikawa, K.; Kurata, N. *Macromolecules* **1992**, *25*, 1588.

(44) Kawaguchi, M.; Sakata, Y.; Anada, S.; Kato, T.; Takahashi, A. *Langmuir* **1994**, *10*, 538.
(45) Melnichenko, Y. B.; Kiran, E.; Heath, K. D.; Salaniwal, S.; Cochran, H. D.; Stamm, M.; Hook, W. A. V.; Wignall, G. D. *J. Appl. Crystallogr.* **2000**, *33*, 682.
(46) Fetters, L. J.; Hadjichristidis, N.; Lindner, J. S.; Mays, J. W. *J. Phys. Chem. Ref. Data* **1994**, *23*, 619.
(47) McMurry, J. *Organic Chemistry*; Brooks/Cole: Belmont, 1992.
(48) Scheutjens, J. M. H. M.; Fleer, G. J. *J. Phys. Chem.* **1980**, *84*, 178.
(49) Bates, F. S.; Fredrickson, G. H.; Hucul, D.; Hahn, S. F. *AIChE J.* **2001**, *47*, 762.
(50) Similarly, the Pt crystallites could be sintered into metal clusters having larger surface areas. This should have the same effect as making bigger individual Pt crystallites.
(51) The initial rate of hydrogenation for toluene could only be estimated, as the rate was too fast to be accurately measured by the digital mass flow controller.

MA010960L